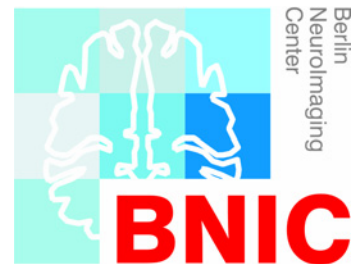


Contrast optimization in functional Nearinfrared-Spectroscopy (fNIRS) by variation of the stimulus-design

Heval Benav

Bachelor's Thesis



INTRODUCTION

Non-invasive imaging-tools for measuring brain activity have attained an important position in various subfields of neuroscience. The most common method – functional magnetic resonance imaging (fMRI) – provides a measurement of the blood oxygenation level-dependant (BOLD) contrast, which depends on changes in regional cerebral blood-flow (rCBF). However, the basic principles of the coupling between the neuronal and the vascular response are still not fully understood (Villringer and Dirnagl, 1995).

The dynamic behaviour of the blood-flow-response to a stimulus can be described by the hemodynamic response function (HRF, Fig. 1). The detailed shape of the HRF is stimulus dependent, but typically starts responding two seconds after a stimulus is presented and reaches its maximum value in the range of 5 to 8 seconds. The response vanishes after 15 to 25 seconds, whereas in some cases a post-stimulus undershoot can be observed (Buxton *et al.*, '98). These values are valid for an arbitrary short stimulus.

The basis of all neuroimaging-methods is the estimation of signal change caused by a change in a stimulus condition, which can be a change in stimulus frequency, attention or computational effort. In the simplest case a stimulus is turned on and off and the different voxels of the brain-image are statistically tested for a significant signal change. To increase the statistical power of the imaging data, the stimulus design (number of stimuli, duration of stimuli, and variance of the duration (jitter)) can be optimized. Several publications deal with this optimization for fMRI data.

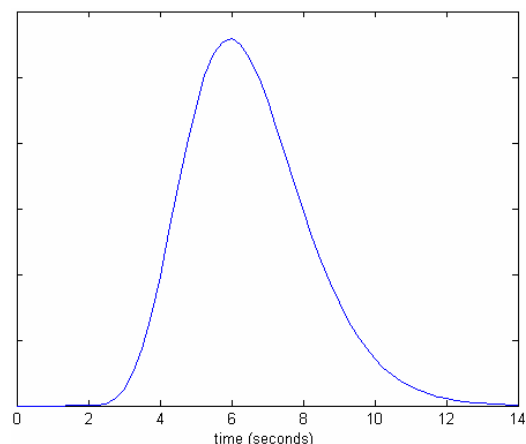


Fig. 1 The hemodynamic response function typically observed neuro-imaging data after a short stimulus

With fNIRS a tool is available returning both the changes in oxy- and deoxyhemoglobin. Its main advantages are the low price and bedside applicability for the price of spatial resolution. Apart from returning two parameters the fNIRS time-course differs from the fMRI signal by a higher sampling rate and potentially a different sensitivity towards the vascular compartments (arteries, capillary bed, veins). Due to these factors the auto-correlation of fMRI and fNIRS data is different and thus a stimulus optimization scheme will return different results for both methods. The following work focuses on optimization of the experimental design of fNIRS studies, since no data has been published so far.

The text at hand mainly deals with the analysis of data acquired by means of fNIRS, an optical approach to measure brain activity. Simulations of stimulus time-courses for variable deterministic experimental designs were generated. Variable deterministic designs were chosen as this sort of occurrence probability is supposed to deliver best results concerning detectability (Friston *et al.*, '99) for fMRI analysis. These stimuli are expected to raise certain specifically shaped hemodynamic responses in rCBF. The responses were produced by convolving the time-course with an ideal HRF kernel, and had been integrated into different kinds of background noise afterwards. The goal was to optimize a significance measure and to relate this optimization to a compound of the stimulus

design, in order to be able to conceptualize appropriate designs for fNIRS procedures with a sampling frequency of 4 Hz. If data is recorded with 4 Hz several influences on the signal have to be eliminated, e.g. the heart beat (app. 0.9 Hz), respiratory changes (0.6 Hz) and other less known biological properties that change the ratio between oxy- and deoxy-haemoglobin, like low frequency oscillations (0.1 Hz), also called V-Waves.

NIRS DESCRIPTION

Data analysis

For most fMRI studies an analysis via a General Linear Model (GLM) is performed. I will now briefly explain the corresponding algorithms and its implementation for the fNIRS data.

In matrix-notation the GLM is expressed in:

$$S = X\beta + \eta$$

The measurable signal time-course S can be calculated as the product of the Design Matrix X , consisting of the experimental design and including some filtering functions, and some unknown parameters in β , plus a noise term η . If the background noise in η is normally distributed one can assume that the data is not influenced by auto-correlation caused by the recording strategy (Friston *et al.*, '99).

Typically, specific paradigms are underlying the experimental design which studies on brain activity are based on. For creating such stimulus time-series two main variables are used. The interstimulus interval (ISI) is defined as the time between the start of two succeeding stimuli. The stimulus duration (SD) determines the time spent in the task state for the stimulus.

On one hand, there are block-like stimulus designs, in this case the shape of a stimulus time-series is regular, with fixed ISI and SD. Changes between different states (ON / OFF) occur equally throughout the complete duration.

The other extreme is provided by event-related (ER) procedures, which allow different trial designs to be randomly intermixed. It is clear that ER procedures highly increase experimental flexibility and the amount of feasible designs, because in this way trials and stimuli can occur in unpredictable randomly shaped sequences. Stimuli can be presented rapidly and correspond to typical behavioural and electrophysiological studies. Furthermore an enhancement for the resulting statistical power is obtained, because more stimuli can be comprised per time-unit.

However, the main limitation for presenting separate rapidly succeeding events is given by the fact that the HRF is delayed in its onset and also evolves over an extended period of time, even for brief neuronal events (Blamire *et al.*, '89).

This problem might be solved using a design with adequate resting states between long task states, in this way the resulting responses cannot overlap anymore (Buckner *et al.*, '93) and are more reliably reconstructable. This solution reduces the choice of possible applicable paradigms though, which is not desirable.

On the other hand an extremely shortened and fixed ISI results in an overlapping of the responses to these stimuli and heavily reduces the quality of measurable signal contrast (Cox & Bandettini, '98, Hutton *et al.*, 98).

The minimum SD (SD_{\min}) is another important property for the shape of the experimental design. A short SD_{\min} leads to stimuli like they would be expected in ER-techniques and raises the chance of

having rapid and numerous changes between task- and resting-state. A higher SD_{min} causes the time-series to expose lengthy ON-periods and corresponds to designs which are more block-like.



Fig. 2 Experimental stimulus designs with varying (2a) and fixed (2b) ISI and SD

The accuracy of estimating the regressor coefficients is given by the corresponding elements of the covariance matrix of X . Hence detectability is defined as:

$$D = \frac{1}{\text{trace}\{(X^T X)^{-1}\}}$$

This definition is set upon values in the Design Matrix X , and is therefore based on the experimental design only. It does not regard the background noise which is contained in the recorded data. Thus detectability is not dependant on any kind of noise in recordings.

The following observations are concentrated on the effect of the average ISI on detection power. Various simulations were made with three different types of measuring the changes in BOLD-contrast.

$$\begin{array}{lll} \text{i)} & \text{ii)} & \text{iii)} \\ z = \frac{\beta}{SEM} \cdot \sqrt{\frac{T}{ISI_{mean}}} & t = \frac{\beta}{SEM} \cdot \sqrt{\frac{T}{f}} \cdot \sqrt{D} & t_{StimDependant} = z \cdot \sqrt{D} \end{array}$$

With duration of the time-course T , and the recording frequency f .

The standard error of mean is defined as:

$$SEM = \sigma_{(\eta)}$$

In i) the results are derived from a z-value expressing how many times SEM the β in the treated voxel differs from SEM.

Both other methods take detectability into account, but in iii) the β is set into relation to ISI_{mean} , hence the number of stimuli that are presented influences the significance of the result.

In contrast to the involvement of the sampling-frequency in ii), which here yields to fact, that the total number of points in the data observed have an influence on the resulting significance measure.

NIRS-Basics

The method can detect concentration changes of chromophores in illuminated tissue. With respect to hemodynamic changes the oxygenated and deoxygenated form of hemoglobin are the principal absorbers to be assessed by NIRS ([oxy-hemoglobin], [deoxy-hemoglobin]). They are differentiated by their different color, i.e. their different extinction spectra $\epsilon(\lambda)$. The physical background is the Beer-Lambert law, stating that the concentration c of a compound is proportional to the attenuation A of light at a certain wavelength ($A(\lambda) \sim c$). To differentiate between various absorbing compounds in the medium, measurements at different wavelengths are required. The number of discrete wavelengths must equal or exceed the number of compounds to be differentiated, to not result in an ill posed problem.

Technically NIRS is rather simple, which is the main prospect for its potential application at the bed-side. Light is injected into the tissue at a certain location on the subject's head with intensity I . Since biological tissue is rather transparent in the spectral range between 650-950 nm, a sufficient amount of photons will reach a depth of about 2-3 cm. Thus the structure of interest, the cerebral cortex, is part of the sampling volume. However, light is strongly scattered by biological tissue. On the one hand the substantial scattering is helpful since some of the light will leave the head in the vicinity of the emitting probe (reflection mode), and thus allows for a rough localization of the data obtained with respect to cortical topography. In this way changes in attenuation measured between the light emitting probe and a detection-probe, attached some centimeters apart, can be ascribed to the cortical region underlying the probe pair.

On the other hand, scatter is assumed to be zero in the standard formulation of the Beer-Lambert law. Biological tissue is a strongly scattering medium and thereby requires modifications of the Beer-Lambert equation. With substantial scattering in the medium, photons which are not detected may have been either absorbed or leave the tissue due to scatter. Since both effects cannot be differentiated and the tissue's scatter properties are not known, the general assumption is that scatter-coefficient (μ_s) is large but constant. The linear term G is therefore added to the Beer Lambert equation to account for a large but constant loss of light intensity due to scatter. Since the magnitude of G is not known only the changes in the attenuation of the tissue can be assessed to derive changes in a compound's concentration c . Besides the term G accounting for the loss of photons due to scatter, a second modification of the Beer-Lambert equation is necessary when applied in scattering media. This is the correction for the fact that the photons detected have traveled a path, which is longer than the geometrical distance between the probes (Fig. 2). Hence quantification of the changes is possible only under the assumption of a constant called "pathlength factor" (Delpy *et al.*, '88). Introducing this factor the modified Beer Lambert law can be derived:

$$A(\lambda) = c \cdot \epsilon(\lambda) \cdot DP(\lambda) + G(\lambda) \quad (1)$$

$$\Rightarrow \Delta A(\lambda) = \Delta c \cdot \epsilon(\lambda) \cdot DP(\lambda)$$

Despite the number of grossly simplifying assumptions this approach is sufficient to detect hemodynamic changes in a cortical area under the probes as is demonstrated in Fig. 3. An imaging pad (5cm x 10cm) consisting of several source and detection fibers was placed over the motor

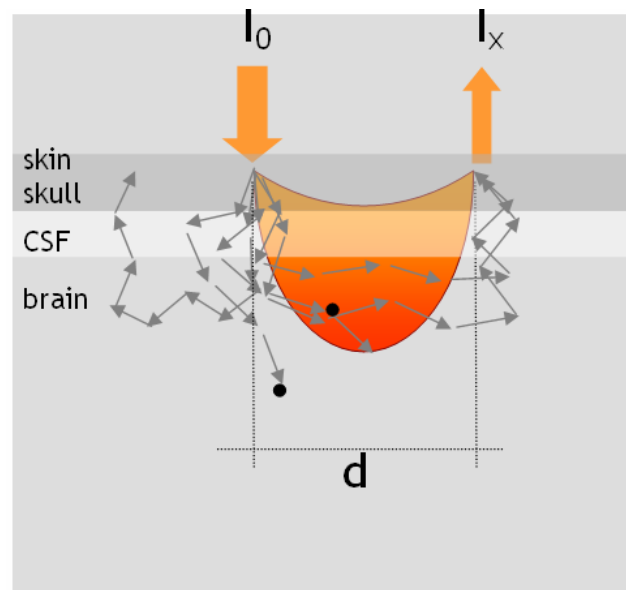


Fig. 2 A sketch of the general principles of NIRS

cortex. During the stimulation period (20s) the subject performed a simple motor task. The left panel shows the event correlated change in oxy- and deoxyhemoglobin which are rather focal.

Fig. 3 also shows the related t-maps, indicating the significant concentration changes due to large amplitudes of the t-value.

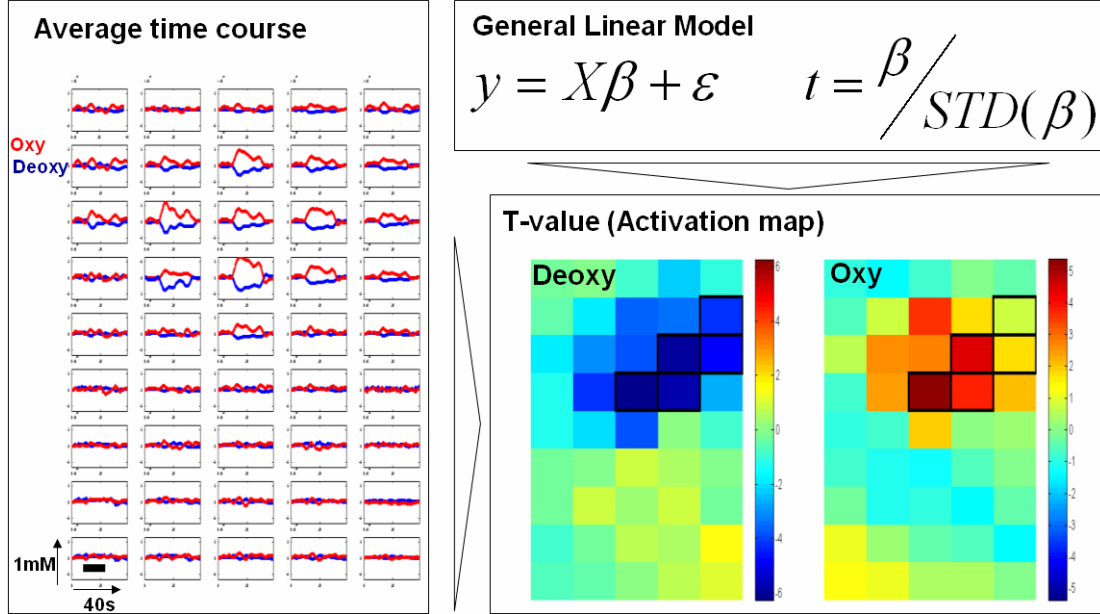


Fig. 3 Application of the GLM to fNIRS-analysis. High values for statistical significance display the location where activation could be reconstructed. Averaged time courses point out the progress of activation in a 9x6 pixel field. The t-map shows an activated area after inducing motor-cortex activity.

METHODS AND SIMULATION

Randomly designed stimulus time-series were generated with varying average ISI as a parameter and a fixed minimum SD. For each time series the relative amount spent in the on state was determined to be 0.5 if possible (it is only possible if the mean ISI is at least twice as large as the mean SD). This fraction of time referred to as the $ratio_{ON}$ of a stimulus time series has strong influence on the detection power, which leads to changes in measurable contrast. The individual ISIs which were needed to generate a stimulus time-series, were randomly distributed according to a truncated Gaussian distribution, with a mean

$$\mu_{ISI} = ISI_{mean} \quad \text{and a variance reaching}$$

$$\sigma_{ISI}^2 = 4 \cdot \log_2 (ISI_{mean})$$

Having defined the individual ISI, a SD was randomly chosen, with respect to the desired $ratio_{ON}$ for each stimulus.

The parameters for the choice of each SD were obtained from a normally distributed random Variable based on:

$$\mu_{SD} = ISI_{mean} \cdot ratio_{ON}$$

$$\sigma_{SD}^2 = 2$$

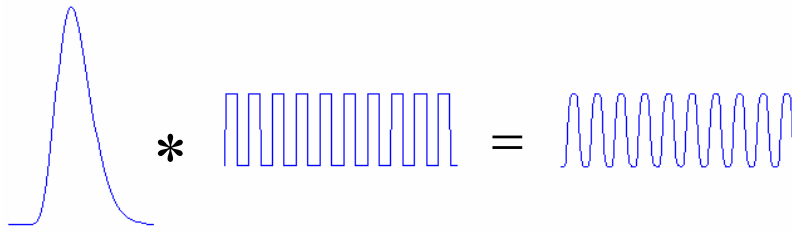


Fig. 4 Convolution of an ideal HRF with a stimulus time-series to a simulated physiological activation response

The HRF with duration of 14 seconds was created using a gamma variate function.

$$HRF(t) = t^{8.6} \cdot e^{-t/0.547} \quad (2)$$

Each stimulus time-series was convolved with this function, to emulate a physiological response (Fig. 4). A convolution can be described as a multiplication in the Fourier domain, i.e. the Fourier transform of the result is equal to the multiplication of the Fourier transform of the input times the Fourier transform of the convolution.

In each simulation a fixed SD_{\min} was determined and the average ISI varied in the range of a certain interval, defined as

$$Interval_{ISI_{mean}} = [SD_{\min} + 0.25s, 10 \cdot SD_{\min}]$$

The start could not be located at SD_{\min} itself, because otherwise $ratio_{ON}$ would have been set to 1, which means 100 % task-state and is not applicable, so the minimal possible amount of time was added. With a sampling frequency of 4 Hz this means 0.25 s.

Background noise was added to the resulting simulated response. In this work two types of noise were evaluated: A) random white noise and B) resting data from fNIRS recording used as a more realistic background. In the latter case the noise has a coloured nature, which means it is not Gaussian normally distributed. The difference of the effects on detection power will be discussed later on.

In physiological circumstances the expected activation amplitude for the [oxy-Hb]-signal is approximately three times larger in its magnitude than for the [deoxy-Hb]-signal (Obrig *et al.*, 1996), hence the given simulated responses were adjusted to deal with the same difference. The measure for significance in detection power, that is reconstructing the activation, is supposed to expose approximately the same difference. By adding the result of the convolution procedure to the background, the simulation of an approximation to activation in brain tissue was completed and could be detected by appropriate procedures.

These procedures are fundamental for analysis of fNIRS data, and include highpass-filtering by a range of different cosine functions, depending on the mean stimulus duration. An existing Matlab[®] program which had been implemented for fNIRS-analysis in our institute was adapted to comply with requirements for analysis of simulated data. In the first step the same HRF was used for simulation and for analysis, which led to high significance values. In real experiments only an estimate of the HRF is available. Quantifying the effect of the incomplete knowledge about the HRF will be part of a follow up work.

RESULTS

Influences of varying fractions spent in the task-state – the optimum $ratio_{ON}$:

In general detectability depends on all parameters characterizing the stimulus time-course. To find out about the influence of $ratio_{ON}$, the detectability was evaluated at an ISI_{mean} of 30s. and SD_{min} of 1, as can be seen in Fig. 5. To calculate the dependence of detection efficiency on $ratio_{ON}$, stimulus time-courses with a fixed ISI_{mean} and SD_{min} were generated (Fig. 5). The most efficient probability is 0.5, which is inline with other results (Friston et al., 99, Birn et al, 2000).

If the amount of time spent in the task state equals the time spent in the rest state, for that time-series detectability can result from a well balanced

difference in both states which have to be compared to each other (Birn *et al.*, 2000). This fact looses in strength in any of both fractions, ON or OFF state take up more time than the other, and as a consequence the explanatory power of the measurable contrast heavily decreases.

Each point in Fig. 5 represents one stimulus time-series and informs about the detectability for this special design. Many designs can be randomly generated, and after the investigation mentioned above, the best one can be chosen for a particular experiment with specific demands.

Having ascertained the optimal fraction to be spent in the task state, in the following simulations $ratio_{ON}$ was always fixed to 0.5. Clearly, this not possible for ISI_{mean} that are larger than $2 \cdot SD_{min}$, and for $ISI_{mean} < 2 \cdot SD_{min}$. In these cases $ratio_{ON}$ was chosen to be as close as possible to 0.5.

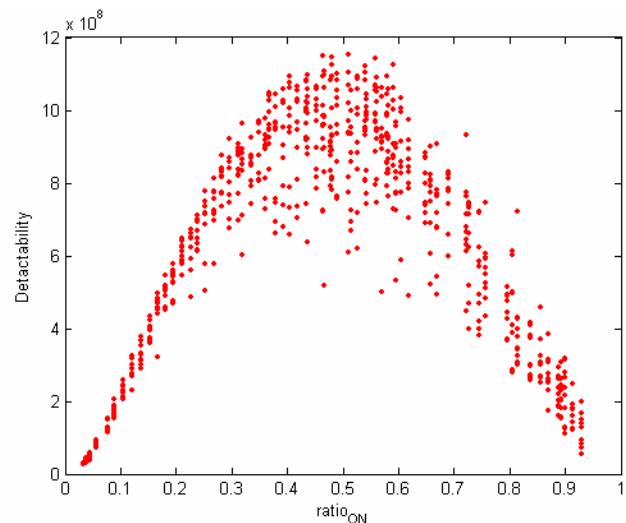
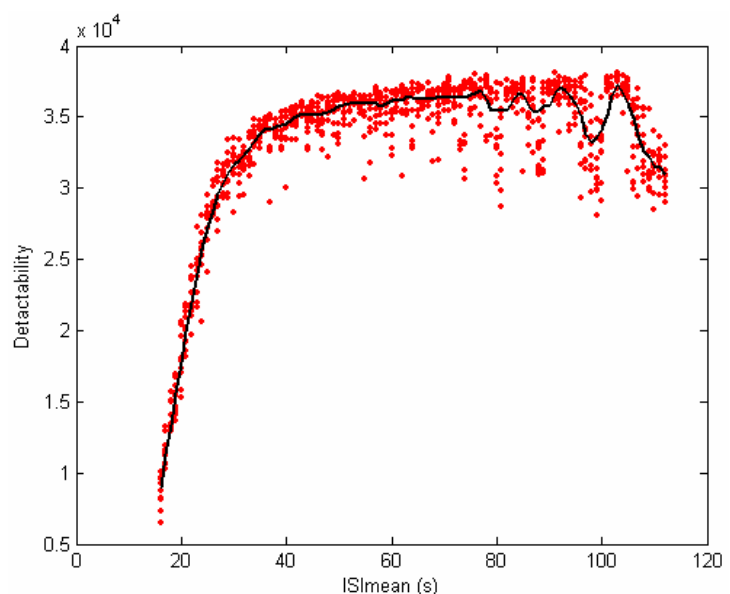


Fig. 5 Detectability of BOLD-changes in a simulation vs. $ratio_{ON}$. Each point represents one time-series. ($SD_{min} = 4$ sec., $ISI_{mean} = 30$ sec.) Detectability is given in arbitrary units.

Fig. 6 Detectability plotted vs. average ISI ($SD_{min} = 16$). For low ISI_{mean} values detectability is quite low, but increases with increasing fraction in task state. For large ISI_{mean} values the results show more variance.



In Fig. 6 the computed detectability is related to the average ISI, for $SD_{\min} = 16$. Detectability increases approximately up to $ISI_{\text{mean}} = 40$, then remains on a constant level, but is showing more variance with increasing ISI_{mean} values. While $ISI_{\text{mean}} < 40$, the ON-fraction continuously decreases from nearly 1 to a value near 0.5, then is held at 0.5, hence a constant level is reached. The visible fluctuations can be explained by the fact that the variance of ISI was related to ISI_{mean} during the simulations, and therefore increases with increasing values.

In order to find the optimum design, all other measures of signal-specificity were also tested (see i), ii) and iii)). : Fig. 7 (A) shows that the z-measure continuously decreases with a growing ISI, due to a smaller number of stimuli being covered by the analysis. Fig. 7 (B) shows the $t_{\text{StimDependant}}$ vs. ISI_{mean} : For short ISI_{mean} the convolution with the HRF leads to small stimulus induced changes in the signal time courses and thus decreases the t-value. The influence exerted by Detectability keeps the measure at low values as well. For larger ISI_{mean} the number of stimuli is strongly decreased, leading to a poor statistical power. This effect is not observable in the t values defined by equation iii) (Fig. 7 C), where the use of only few stimuli returns the optimum statistical power. This indicates the problems coming up with this parameter, which is simply a linear mapping of Detectability and therefore does not comply with the requirements dealt with in this work.

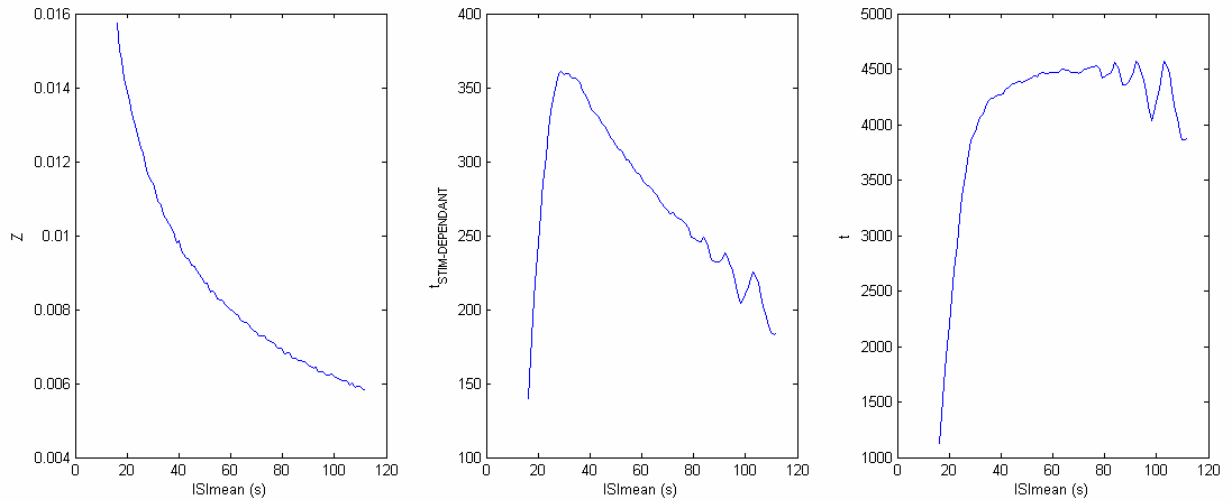


Fig. 7 Comparison of applied significance measures: z , t , and $t_{\text{Stim-Dependant}}$. Data only shown for deoxyhemoglobin (absolute values)

The measure in ii), $t_{\text{StimDependant}}$, was used in all further simulations and is supposed to deliver useful results concerning an optimal experimental design.

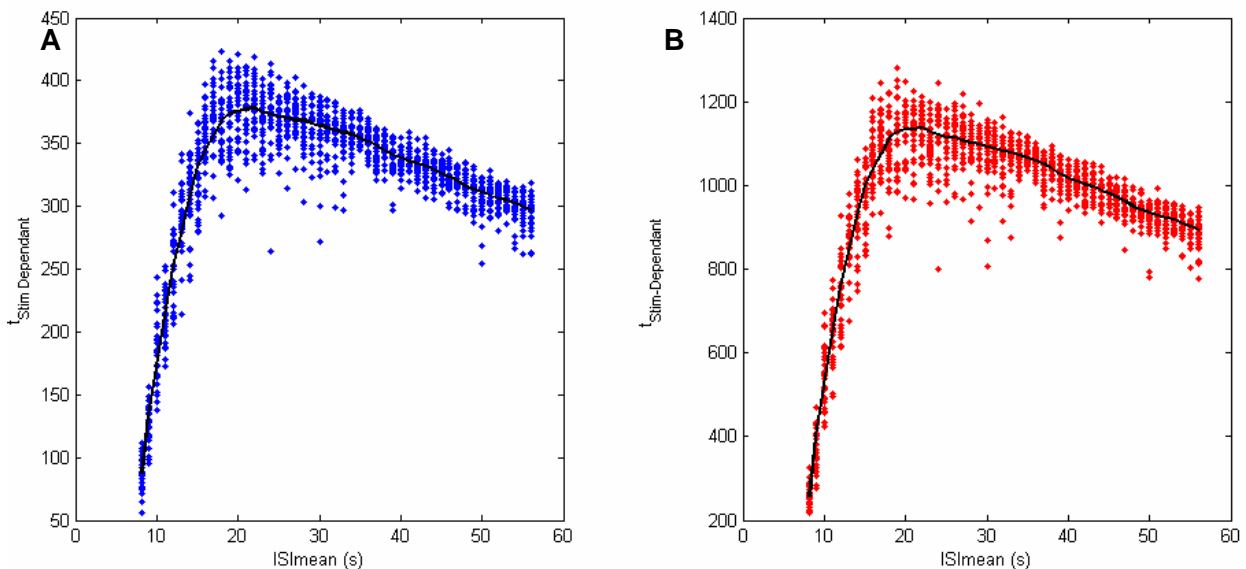


Fig. 8 Relation between the average ISI and $t_{\text{StimDependant}}$ for deoxy- (A) and oxy-haemoglobin (B). The solid line represents the median values for all simulations. (Absolute values plotted for deoxy)

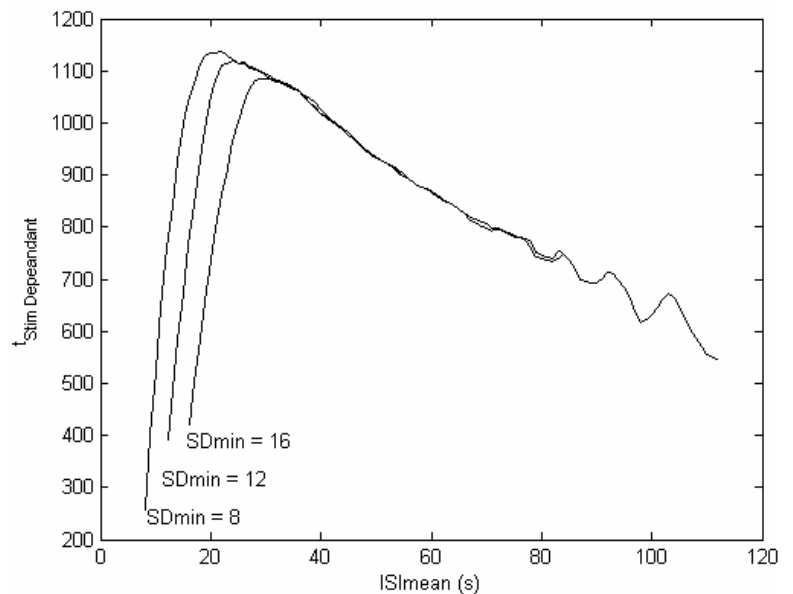
With a white noise background from random data the amplitude of $t_{\text{StimDependant}}$ in the oxy-signal is three times larger than for the deoxy-signal (Fig. 8). For an $SD_{\text{min}} = 8$ s the signal peaks at $ISI_{\text{mean}} \approx 16$ s., and reaches lower values again for longer average ISI durations. The maximum located at $2 \cdot SD_{\text{min}}$ is reasoned by the optimal fraction for $ratio_{\text{ON}}$ and by concurrently involving a large number of stimuli into the experimental design.

The $t_{\text{StimDependant}}$ values for [oxy-Hb] triple [deoxy-Hb] as expected from the induced concentration changes.

The next question was concentrated on how different minimal SD durations influence the measurable contrast. Simulations dealing with this question were performed by setting SD_{min} to 8, 12 and 16.

Fig. 9 Plot for $SD_{\text{min}} = 8, 12$ and 16

The plot of $t_{\text{StimDependant}}$ reaches its maximum value at $2 \cdot SD_{\text{min}}$ for each of the three different SD_{min} . With increasing SD_{min} the peak value decreases. For growing ISI_{mean} the results are equal in each case



In Fig. 9 an averaged $t_{\text{StimDependant}}$ ($n = 10$) is plotted for each of the three different SD_{min} values versus ISI_{mean} . The attitude for different minimal SDs in Fig. 9 underlines the sensitivity of $t_{\text{StimDependant}}$ to the amount of presented stimuli. Longer average ISI durations result from a higher SD_{min} , and therefore the time-series which contains 2000 data points, with a sampling frequency constituting 4 Hz, delimits the presentable number of stimuli. Thus for $ISI_{\text{mean}} = 100$ about 5 stimuli only can influence the statistics. For very long ISI durations the results are equal, because the influence SD_{min} has on the ratio for the simulations vanishes and a task-fraction of 50 % is reached in each case, not dependant on SD_{min} anymore.

The maximum value for the t value and for $t_{\text{StimDependant}}$ is a function of the minimal stimulus duration, for t it is located at $2 \cdot SD_{\text{min}}$ (Birn *et al.*, 2000). For this ISI duration an average stimulus has at least a $ratio_{\text{ON}}$ of about 50 %, which corresponds to high detectability as could be shown. For longer ISI_{mean} durations $ratio_{\text{ON}}$ could decrease, but was held at 50 % in these simulations. The Detectability measure decreases anyway, because of a decreasing number of presentations which could strengthen the explanatory power.

For very short SD_{min} comparisons the detectability increases with a growing SD_{min} , because the experimental design in a time-course with $SD_{\text{min}} = 1$ is much more Event Related than in one with $SD_{\text{min}} = 4$, where the design appears to be more block-like (Birn *et al.*, 2000). This influence is not observable anymore for values in a range between 4 and 16. Very short average ISI durations are hardly to reconstruct and heavily influence reliability on the results, because overlapping of single responses occurs throughout the whole duration of the time course.

EFFECTS OF REAL BACKGROUND DATA:

If the background is described by real fNIRS data from 4 Hz recordings the results do not exhibit the same behaviour anymore. The results provide a maximum that is located near $2 \cdot SD_{min}$ (Fig. 10), but with increasing ISI_{mean} the measure does not decrease as clearly as for a random background. The resting data acquired by fNIRS are susceptible concerning artefacts caused by movement of the person or supplementary light which intrudes the skull from other sources except the light emitting diodes.

In addition, physiological oscillatory fluctuations in the [oxy-Hb] signal are much larger than in the deoxy-signal (Respiration, Heart Beat, V-waves). This leads to data with even more intrinsic variance for the oxy-signal. Therefore, although a oxy-response is integrated which triples the size of the deoxy-response, $t_{StimDependant}$ is of the same magnitude.

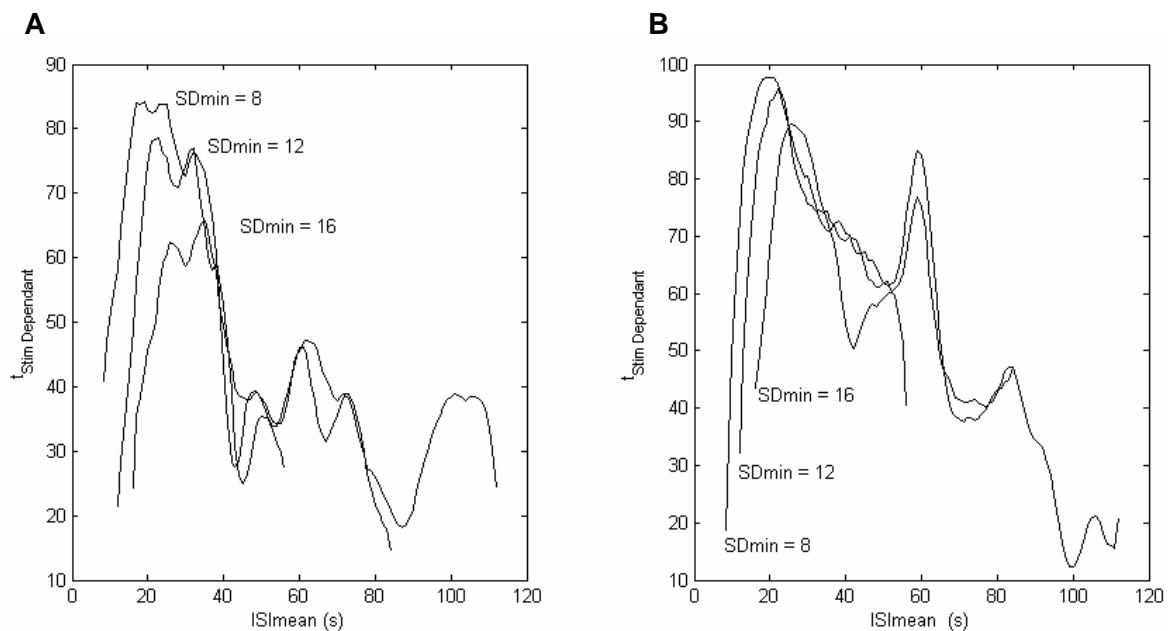


Fig. 10 In these simulations the background noise was described by fNIRS-resting data, which had been filtered by a high *pass*-filter. The measurable contrast for oxy-signal is only slightly higher than in deoxy, due to a higher variance concerning measurable [oxy-Hb]-changes. Plot for $SD_{min} = 8, 12, 16$ (Smoothed data plotted, averaged values)

SIMULATIONS WITH VARYING HEAMODYNAMIC RESPONSE FUNCTIONS

All simulations so far assumed the given gamma-variate function (2) as representing the HRF. Because this is not likely to mirror the variance which is expected to occur in the human brain, this assumption was extended to a range of different HRFs, based on slightly varying the exponential factor for the gamma-variate function (2). Five different functions were used during simulations, whereas the procedure for analysis of this data still dealt with only one HRF (Fig. 11).

Fig. 11 shows that the determined $t_{StimDependant}$ scatter over a large range of values. The median (black line) shows a less pronounced peak as in the results above. Also the peak appears earlier.

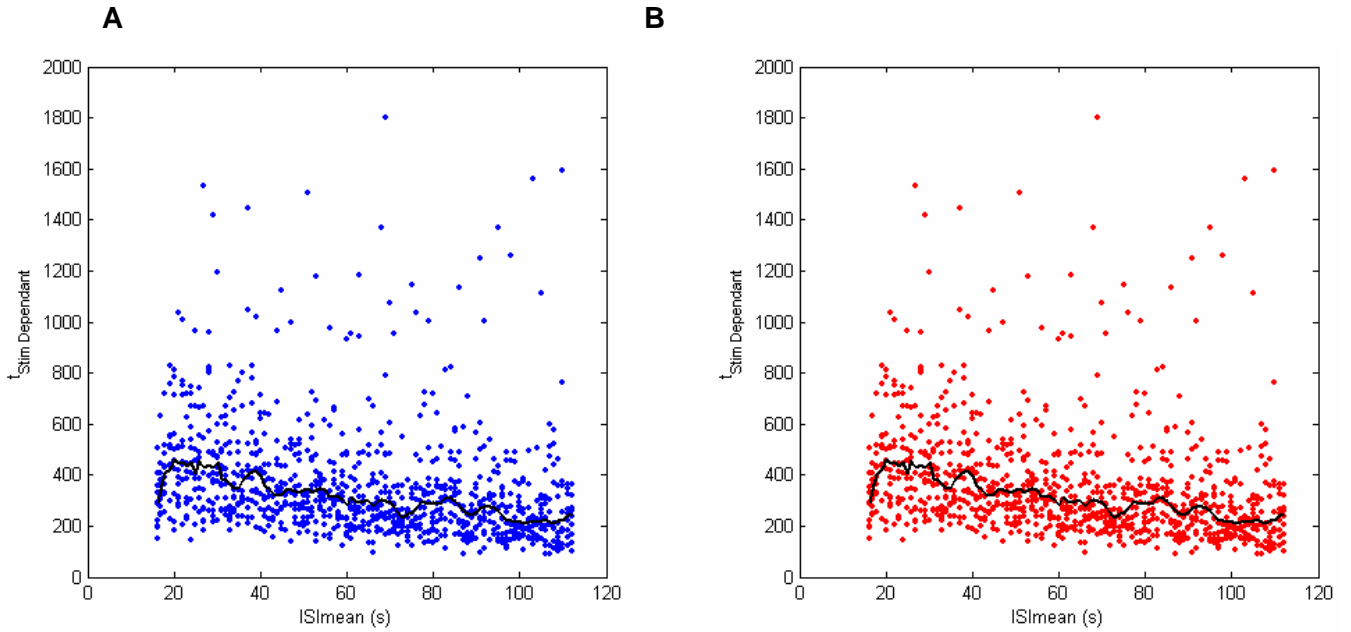


Fig. 11 Results obtained with 5 different randomly chosen HRF functions. All measures exposed a higher variance than for a simple HRF. (deoxy in A, oxy in B) ($SD_{min} = 16$, absolute values for deoxy)

SUMMARY AND DISCUSSION

In this work four different significance-measures which quantify the quality of reconstruction of induced simulated stimuli were investigated. The z-measure delivered very high significances for experimental designs with a large number of presented stimuli, whereas detectability and the t-measure did not take into account the total number of stimuli and remained constant for a constant ratio_{ON}. Thus we considered $t_{StimDependant}$ for further efficiency evaluations.

Regarding $t_{StimDependant}$ over ISI_{mean} a maximum can be found (Fig. 9). This maximum is always located at $2 \cdot SD_{min}$, the amplitude of the maximum decreases with rising SD_{min} , indicating the advantage of single-trial designs over blocked designs. This means, to exploit these effects for the choice of a certain experimental design in a fNIRS-study, the minimal SD has to be fixed at a low value for a certain time-course, e.g. $SD_{min} = 4$. In order to optimize the contrast, durations of presented stimuli in that experiment are supposed to average 8 or some slightly larger value.

For simulations on random Gaussian background data the peak $t_{StimDependant}$ -values for [oxy-Hb] were three times larger than for [deoxy-Hb], equal to the induced difference (Compare Fig. 8 (a) and (b)). This behaviour was not as straightforward when background noise from real data was applied, because of larger variations in recordable oxy-data in fNIRS. This leads to the understanding that physiological changes in [oxy-Hb] might be even larger, but cannot be reconstructed in their original amplitude, due to the influence of highly varying data on statistical significance.

Utilizing fNIRS time-courses as background-data, the $t_{StimDependant}$ -measure exhibits additional deflections for growing ISI_{mean} (Fig. 10), these local peaks are caused by low-frequency-oscillations in the cerebral blood-flow.

Changes in rCBF, caused by a stimulus, are commonly approximated by a HRF, which varies between stimuli and subjects. For the data in Fig. 11 we simulated an expected stimulus-to-stimulus variance. Induced hemodynamic changes have a less pronounced peak at shorter ISI_{mean} . This has large implications on the optimal stimulus design where short ISI_{mean} values would be favoured.

REFERENCES

- Birn RM, Cox RW, Bandettini PA.
Detection versus estimation in event-related fMRI: choosing the optimal stimulus timing.
Neuroimage. 2002 Jan; 15(1):252-64.
- Blamire AM et al.
Proc Natl Acad Sci USA 89, 11069-11073 (1992)
- Buxton RB, Wong EC, Frank LR.
Dynamics of blood flow and oxygenation changes during brain activation: the balloon model.
Magn Reson Med. 1998 Jun; 39(6):855-64.
- Cox RL and Bandettini PA.
Proc Int Soc Magn Reson Med Sixth Sci Meetin, Exhib 1, 244 (1998)
- Delpy DT, Cope M, van der Zee P, Arridge S, Wray S, Wyatt J.
Estimation of optical pathlength through tissue from direct time of flight measurement.
Phys Med Biol. 1988 Dec, 33(12):1433-42.
- Friston KJ, Zarahn E, Josephs O, Henson RN, Dale AM.
Stochastic designs in event-related fMRI.
Neuroimage 1999 Nov; 10(5):607-19.
- Hutton et al.
Proc Int Soc Magn Reson Sixth Sci Meeting Exhib 2, 1430 (1998)
- Obrig H, Wolf T, Doge C, Hulsing JJ, Dirnagl U, Villringer A.
Cerebral oxygenation changes during motor and somatosensory stimulation in humans, as measured by near-infrared spectroscopy.
Adv Exp Med Biol. 1996; 388:219-24.
- Villringer A, Dirnagl U.
Coupling of brain activity and cerebral blood flow: basis of functional neuroimaging.
Cerebrovasc Brain Metab Rev. 1995 Fall; 7(3):240-76. Review